RI 8045

Bureau of Mines Report of Investigations/1975

Low-Temperature Heat Capacities and Enthalpy of Formation of Copper Oxysulfate

UNITED STATES DEPARTMENT OF THE INTERIOR

Report of Investigations 8045

Low-Temperature Heat Capacities and Enthalpy of Formation of Copper Oxysulfate

By J. M. Stuve, D. W. Richardson, and E. G. King
Albany Metallurgy Research Center, Albany, Oreg.

UNITED STATES DEPARTMENT OF THE INTERIOR
Rogers C. B. Morton, Secretary

Jack W. Carlson, Assistant Secretary–Energy and Minerals

BUREAU OF MINES
Thomas V. Falkie, Director

This publication has been cataloged as follows:

Stuve, John M

Low-temperature heat capacities and enthalpy of formation of copper oxysulfate, by J. M. Stuve, D. W. Richardson, and E. G. King. [Washington] U.S. Bureau of Mines [1975]

18 p. illus., tables. (U.S. Bureau of Mines. Report of investigations 8045)

Includes bibliography.

1. Copper oxysulphate. I. U.S. Bureau of Mines. II. Richardson, Dale W., jt. auth. III. King, Edward G., jt. auth. IV. Title. (Series)

TN23.U7 no. 8045 622.06173

U.S. Dept. of the Int. Library

CONTENTS

ILLUSTRATIONS

TABLES

LOW-TEMPERATURE HEAT CAPACITIES AND ENTHALPY OF FORMATION OF COPPER OXYSULFATE

by

J. M Stuve,[1] D. W. Richardson,[2] and E. G. King[3]

ABSTRACT

Low-temperature heat capacities and the enthalpy of formation were determined calorimetrically by the Bureau of Mines for $CuO \cdot CuSO_4$. The derived standard entropy ($S^\circ_{298.15}$) was 40.36±0.04 cal/deg-mole, and the enthalpy of formation ($\Delta H^\circ f$) was -219.1±0.3 kcal/g-mole. A large thermal anomaly was observed in the heat capacity of $CuO \cdot CuSO_4$ at 20±0.1 K. Gibbs energy of formation data are tabulated up to 1,200 K.

Construction details of a precision low-temperature adiabatic calorimeter capable of determining heat capacities of solids in the temperature range 5 to 320 K are given. A calibrated miniature germanium resistance thermometer was incorporated into the calorimeter to extend the range of accurate measurements below 15 K. High-resistance dc heater windings were used throughout the cryostat to reduce heat conduction of inner connecting wires.

INTRODUCTION

The purpose of this Bureau of Mines investigation was to accurately determine thermodynamic parameters of delerophanite, or copper oxysulfate ($CuO \cdot CuSO_4$), an important component of the copper-oxygen-sulfur system. The standard entropy at 298.15 K was derived from heat capacity data obtained using a recently constructed, adiabatic, low-temperature calorimeter. A detailed description of this calorimeter and its operation in the temperature range 5 to 320 K is given. In addition, heat of solution data were determined with a precision isothermal-jacket calorimeter in a hydrochloric acid solvent. High-temperature enthalpy data by this laboratory were recently reported by Ferrante (3).[4] No previous similar low-temperature heat capacity data for copper oxysulfate were found in the published literature.

---

[1] Research chemist.

[2] Research chemist (now retired).

[3] Supervisory research chemist.

[4] Underlined numbers in parentheses refer to items in the list of references at the end of this report.

ACKNOWLEDGMENTS

The authors are indebted to Professor E. F. Westrum, Jr., of the University of Michigan, Ann Arbor, Mich., for generously supplying considerable basic information relating to construction and operation of low-temperature adiabatic calorimeters, and to Dr. J. P. Chan of the Lawrence-Livermore Laboratory, University of California at Berkeley, Calif., for the initial design of the cryostat. Professor W. F. Giauque of the University of California, Berkeley, Calif., made valuable suggestions during the design stage.

MATERIAL

The sample of copper oxysulfate ($CuO \cdot CuSO_4$) was prepared by thermally decomposing reagent-grade copper sulfate at 725° C for approximately 6 hours. The X-ray powder diffraction pattern of the resulting product agreed with the ASTM listing for $CuO \cdot CuSO_4$. Copper was determined by thermally decomposing the $CuO \cdot CuSO_4$ product to CuO, followed by hydrogen reduction and weighing as metallic copper. The sulfate was precipitated and weighed as barium sulfate. These analyses agreed closely with the theoretical stoichiometry of $CuO \cdot CuSO_4$. Emission spectrographic analysis revealed no significant metallic impurities. Separate portions of the same oxysulfate preparation were used for the low-temperature and solution calorimeter measurements.

LOW-TEMPERATURE CALORIMETRY

Cryostat

The cryostat of the low-temperature heat capacity calorimeter is shown in figure 1. The outermost wall of the cryostat is a chrome-plated brass cylinder terminated at the top by an O-ring flange supporting the lid. All of the internal components of the cryostat are suspended from this lid. Access to the interior is accomplished by lifting the lid assembly with an overhead hoist.

The cryostat is evacuated by a vacuum system coupled to the base of the outer wall by flexible metal bellows. Directly below the bellows is a vacuum-gate valve mounted on a water-cooled 10.2-cm vacuum-diffusion pump. The pressure in the cryostat is monitored with a discharge vacuum gage attached to the lid.

Liquid nitrogen was stored in the upper tank (3-liter capacity), and liquid helium was stored in the lower tank (1.5-liter capacity). Both vessels are constructed of copper and are fitted with circular-base brackets for attaching their respective shields. The fill-pipes are 12.7-mm OD (0.3-mm wall) stainless steel alloy, and the vent tubes are 6.4-mm OD of similar composition. The vent tubes for the liquid nitrogen reservoir are not shown in figure 1. The vent tube for the liquid helium reservoir has a heat exchanger similar to that described by Westrum (16). The exiting cold helium gas is used in this device to reduce heat conduction through the electrical leads between the liquid nitrogen and liquid helium reservoirs. These vessels can be evacuated either singly or together, with a high-capacity rotary pump.

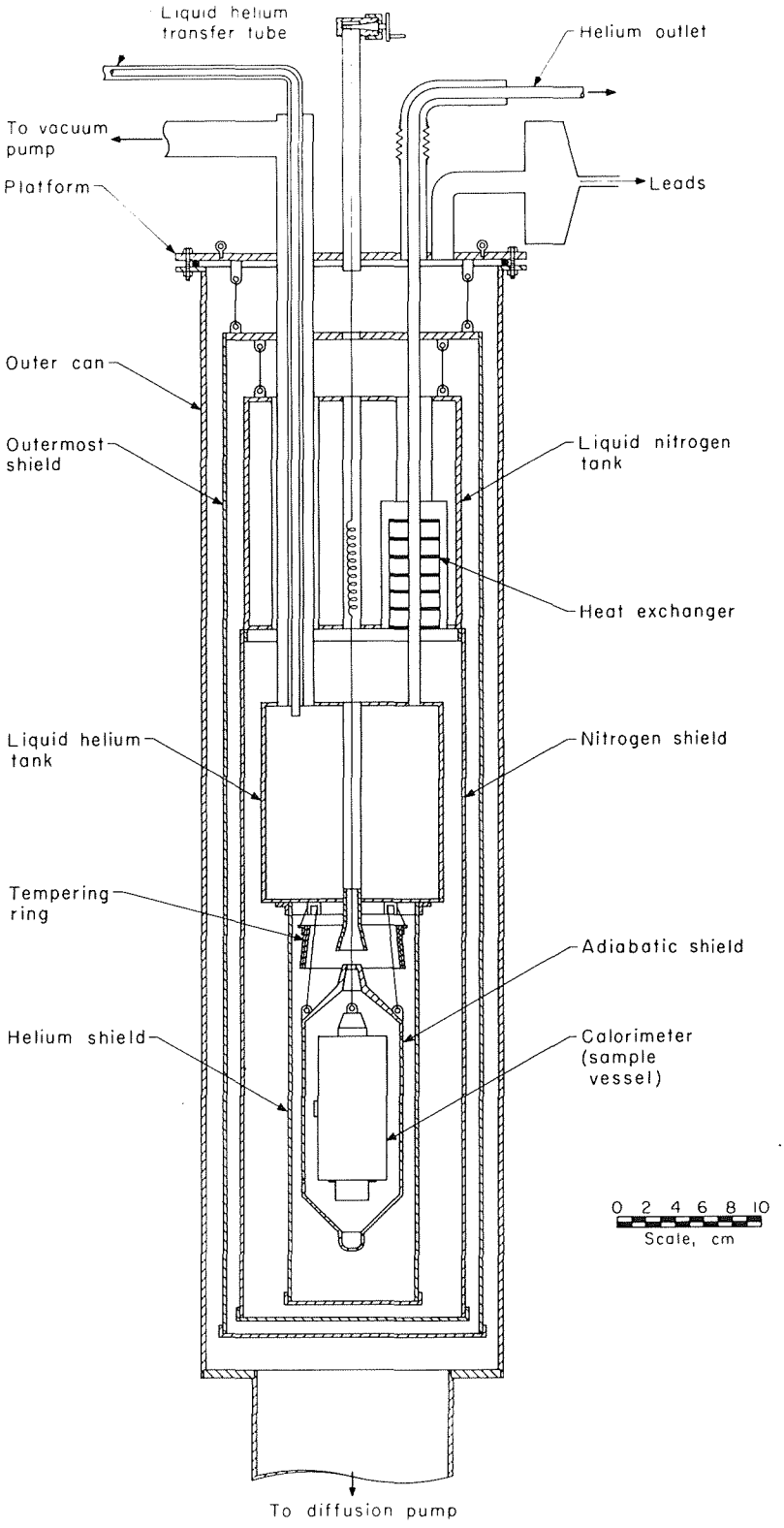

FIGURE 1. - Helium cryostat assembly.

Cryostat temperatures in the range 50 K to ambient are obtained using liquid nitrogen or solid and liquid nitrogen at reduced pressure. Temperatures below 50 K are achieved by filling the lower tank with liquid helium. The liquid helium is transferred into the bottom reservoir by a vacuum-insulated stainless steel tube. One filling of liquid helium (1.5 liters) lasts approximately 20 hours in a precooled cryostat with all heater circuits off.

The calorimeter (sample container) is suspended by a silk line from a winch assembly mounted on the lid of the cryostat (fig. 1). The winch has a turns counter fitted to the shaft for accurate vertical positioning of the calorimeter within the cryostat. The calorimeter is cooled by raising it to provide good thermal contact with the adiabatic shield, which in turn is raised to engage the heat-conduction cone protruding downward from the base of the helium reservoir. When lowered again into the measuring position, the calorimeter and adiabatic shield are thermally isolated from the other cryostat components, except for necessary electrical leads and silk suspension threads.

There are three cylindrical radiation shields concentrically mounted at different elevations within the cryostat. The outermost is the primary radiation

shield and is suspended to isolate it from the remaining cryostat assembly. The nitrogen and helium shields are attached to their respective reservoirs, thereby extending those temperatures into isothermal zones. These shields are copper, plated with gold, finished to a highly polished surface. All of the metallic components within the cryostat have similar plating and finish except the stainless alloys and fasteners.

Electrical wiring is introduced into the cryostat by a sealed multiple feedthrough positioned on the lid exterior (fig. 1). The various heater circuits within the cryostat were designed to use relatively high voltage (100-200) dc instrumentation. Accordingly, some benefit is realized in reducing spurious heat leaks by selecting small wire sizes for current conductors. All cryostat heater leads are 0.127-mm-diam Teflon[5]-insulated copper wire. The heater windings for control shields were wound with Karma, a high-resistivity alloy that has a very small thermal coefficient of resistivity. Critical adiabatic control thermocouples were made from a specially selected 0.127-mm-diam Teflon-coated alloy of Au with 0.07 at. pct Fe paired with premium-grade Chromel P wire of the same size. The thermal power (Seebeck coefficient) of this combination is relatively high and has good reproducibility in the temperature range 5 to 80 K (12). Calibrated copper-constant (type T) thermocouples were used to monitor temperatures of the nitrogen and helium reservoirs and the tempering ring. These thermocouples were also of 0.127-mm-diam Teflon-insulated wire. Each thermocouple pair is routed in a continuous segment and terminated at an external ice-thermostated reference junction.

Calorimeter

The calorimeter (fig. 2) was constructed of high-purity, oxygen-free copper and has an enclosed volume of approximately 90 cm^3. The empty calorimeter with the sealing device, thermometers, and heater unit in place weighed about 90 g. The inside and exterior surfaces of the calorimeter, conduction cone, and thermometer-heater cover are all gold-plated.

The platinum thermometer-heater winding base fits into a well, coaxially positioned, and open at the calorimeter base. The calorimeter is filled and sealed at the central opening below the sealing disk on its lid. Three tin copper conduction vanes in the form of cylindrical loops were tangentially attached to the outer surface of the heater well and terminated at the outer shell of the calorimeter. These vanes aid in the rapid dispersal of heat from the central well into the sample.

The copper heater winding base was wound with a 3,880-ohm (300 K) wire, 0.061 mm in diam, made of Pt-8 at. pct W and insulated with enamel. The outer perimeter of the winding was covered with a thin coating of metallized epoxy resin to protect the insulation and give a close sliding fit into the heater well. The platinum-tungsten alloy heater wire has a thermal resistivity coefficient of about 24 ppm/K in the range 4 to 320 K.

[5]Reference to specific brand names does not imply endorsement by the Bureau of Mines.

The thermometer-heater cover reduces radiative losses from the heater thermometer assembly and also serves as a temperature equalizer for electrical leads leaving the calorimeter. The current and emf leads of the platinum thermometer are 0.10-mm-diam copper wire with enamel insulation. The germanium resistance thermometer current and potential leads are 0.081-mm-diam copper wire. The thermocouple well shown in figure 2 is the point of attachment for the primary adiabatic shield control sensor discussed in the following paragraph.

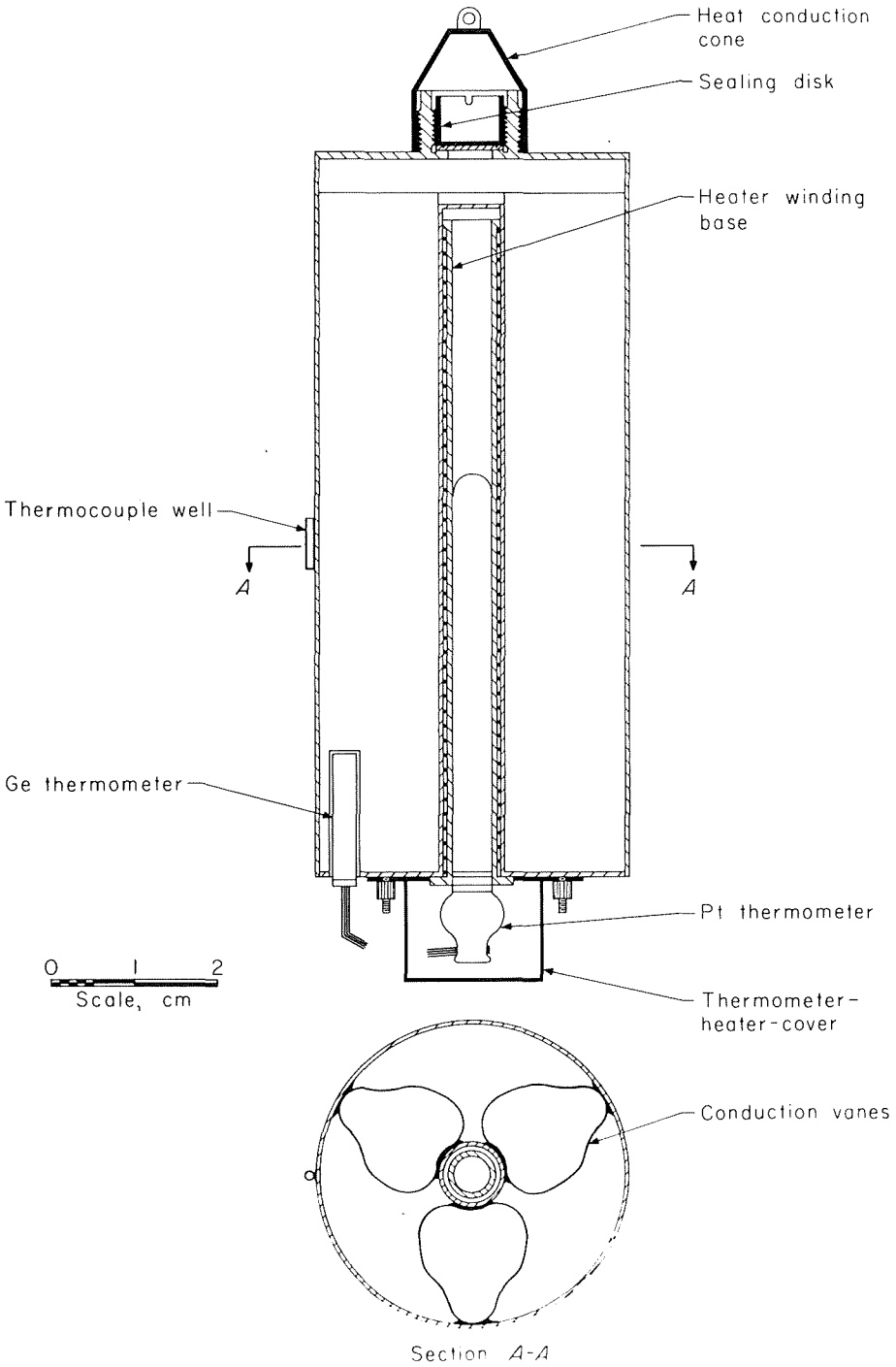

FIGURE 2. - Low-temperature calorimeter.

The calorimeter sealing disk was machined from a stainless steel alloy. The bottom of the disk has a circular knife edge extending slightly below the bottom plane. A thin disk of soft-annealed gold forms a vacuum-tight seal between the knife edge and a smooth circular surface machined around the circumference of the filling orifice. The calorimeter can be loaded and sealed in a helium-filled vacuum dry

box for measurement of air-sensitive materials. Normally the calorimeter is sealed with a reduced pressure of 2 to 5 cm absolute of helium gas to facilitate thermal conduction within the sample calorimeter assembly.

Thermometry

The primary temperature calorimetric reference in the range 15 to 320 K is a capsule-type platinum resistance thermometer that was calibrated at the National Bureau of Standards. It has a nominal 25-ohm resistance at the ice point. The calibration of this thermometer is in terms of the International Practical Temperature Scale of 1968 (IPTS68) (1, 11). Temperature measurements below 15 K are determined by a small helium-filled germanium resistance thermometer. This thermometer was also calibrated at the National Bureau of Standards in the range 2 to 20 K in terms of the National Bureau of Standards Provisional Scale 2 to 20 K (1965).

The resistance of the thermometers was determined potentiometrically using the conventional four-lead, constant-current technique. Direct-current voltages were measured with a Honeywell-Rubicon six-dial double-microvolt potentiometer. This instrument is of low-thermal-emf design and has two measurement ranges: 0 to 111,111.1 μV in steps of 0.1 μV, and 0 to 11,111.11 μV in steps of 0.01 μV. A Keithley model 180 null detector was used to determine the off-null voltages, giving a practical lower limit of ±0.02-μV resolution in the potentiometric measurements. The thermometer current was adjusted to a precise reference value immediately prior to observing the voltage drop across the thermometer for a given temperature reading. A relatively large "ballast" resistor in series with the thermometer minimizes thermometer current drift during the short interval between current adjustment and reading the thermometer voltage. The resistance of the platinum thermometer is nominally 28.1 ohms at 298 K, decreasing to about 0.0418 ohm at 15 K. When a standard reference current of 2.0 mA is used, the voltage-temperature sensitivity is approximately 202 and 16 μV per degree at 298 K and 15 K, respectively. By comparison, the germanium thermometer has a nominal resistance at 5 K of 915 ohms, decreasing to 61.9 ohms at 15 K. With a standard reference current of 10 μA, its voltage-temperature sensitivity was nearly 4,400 μV per degree at 5 K, and 80 μV per degree at 15 K.

Provision was made for reversing the thermometer current and its potentiometer leads to reduce the possibility of thermal emf errors in temperature determinations. All of the critical current reference resistors and the standard cell for the potentiometer were calibrated against laboratory standards traceable to the National Bureau of Standards. A maximum error of ±0.01 K deviation from the IPTS68 was estimated in the temperature range 15 to 320 K for the potentiometer-platinum thermometer system. However, the resolution in measuring temperature difference during a heat capacity determination was of the order ±0.0002 K above 20 K.

Energy Calibration

During a heating period, the energy input to the thermally isolated calorimeter assembly was measured by monitoring the voltage across the heater

winding with a Hewlett-Packard model 2401C integrating digital voltmeter. This instrument measured the volt-second product across the heater winding to a minimum resolution of 1 part in 100,000 with an error of 0.03 percent or less. A choice of measuring ranges could be selected from 100.000-mV-sec to 100.000-V-sec full-scale, thus allowing good resolution for various heater voltage requirements. Input impedance was 100 kilohms on the most sensitive range, increasing to 10 megohms on the 100.000-V-sec range. Corresponding corrections were applied to volt-second products, as necessary, to compensate for the small current in the measuring leads of the integrating digital voltmeter. The internal calibrated time base had a variation of ±2 ppm per week. The heater current was determined potentiometrically by a calibrated standard resistor in series with the heater. A stabilized dc source maintained the heater current essentially constant during the calibration period. The short-term stability of this supply was on the order of 50 ppm for currents in the range 0.1 to 25 mA.

Shield Controls

Temperature regulation in the critical region surrounding the calorimeter was achieved by four precision analog control circuits. Each of these circuits has five basic components: a differential thermocouple input, a high-gain bipolar dc amplifier (null detector), a current adjusting-type (CAT) controller, a dc power amplifier, and a resistance heater winding.

The lead bundle approaching the adiabatic shield was preheated on the tempering ring assembly (fig. 1). The control sensor in the tempering ring circuit is a copper-constantan thermocouple of 0.127-mm Teflon-insulated wire. The heater windings of all the control circuits are made of 0.11-mm, silk-insulated Karma wire. These windings were cemented in a helical pattern on the shield surface with General Electric type 7031 adhesive varnish.

The adiabatic shield was suspended below the tempering ring with silk threads. It is fabricated in three copper sections each with a separate temperature control channel. The cylindrical center element is the primary control zone. The temperature of this section was made subordinate to the calorimeter by attaching one leg of a differential thermocouple to the inner surface of the shield section and anchoring the outer end to the outer surface of the calorimeter. The μV deviation of this sensor (Chromel P--Au with 0.07 at. pct Fe) was amplified by a Keithley 147 nanovolt null detector, and the analog output signal drove a CAT controller. The output of this device was coupled to a variable-gain operational power supply, which in turn energized the heater winding, thus completing the control loop. The usable temperature sensitivity of this shield control circuit was about ±0.001 K in the range 10 to 320 K. An important feature of this circuit is an adjustable dc bias voltage at the null detector input stage to balance the control point of the shield thermocouple to adiabatic conditions prior to heat capacity measurements.

Temperature controls of the shield end zones were trimmed to closely follow the center-zone temperature. The CAT controller, with variable proportional band and reset, allowed optimum control over a wide range of shield

load conditions. Temperature deviations of all control circuits from the adiabatic control point were visually monitored on analog-strip recorders during the course of measurements.

The only significant "bumps" in the control circuit deviation traces occurred during brief intervals after the calorimeter heater was turned on or off. The recorded temperature deviations, during these transient periods, were generally symmetric and opposite in direction; thus they tended to minimize the net heat exchange of the calorimeter with its surrounding shield within a given measurement period.

Measurements and Results

The heat capacity of the empty calorimeter was carefully determined in the temperature range 5 to 320 K. A small amount of helium gas was used to improve conduction in the calorimeter. Vacuum grease served the same purpose in the thermometer-heater well. In subsequent heat capacity measurements the quantities of helium and grease were carefully duplicated or corrected to maintain the constancy of the empty calorimeter calibration. The heat capacity at constant pressure (Cp) at a given temperature was determined from the difference between the filled and empty calorimeter heat capacities.

In the present investigation the calorimeter was filled with a 0.30136-g-mole sample of $CuO \cdot CuSO_4$. The sample weight was determined to an accuracy of ±0.5 mg by weighing the filled and empty calorimeter using a large-capacity double-pan analytical balance and calibrated brass weights. The mole weight of $CuO \cdot CuSO_4$ was calculated as 239.149 using the 1969 IUPAC table of atomic weights (5-6). Before loading into the cryostat, the calorimeter was evacuated and sealed with a 25-torr helium pressure at 296 K. The sealed calorimeter was preheated several hours at 318 K in an evacuated cryostat to outgas the assembly prior to cooling.

The $CuO \cdot CuSO_4$ was initially cooled to 77 K, and the first series of heat capacities were taken up to room temperature. These measurements were accomplished in a series of contiguous runs; that is, the initial temperature of one measurement was the final temperature of the previous, until the required range of temperature was completed. The temperature increment covered by a single measurement was scaled to approximately 10 percent of the absolute sample temperature below 120 K. Above this temperature range the measurements were limited to a maximum of about 12 K, using an average heating rate of approximately 0.75 K/min. In the region of the thermal anomaly of $CuO \cdot CuSO_4$ at 20 K, temperature increments on the order of 0.1 K were used to achieve satisfactory resolution.

A typical heat capacity determination consisted of the following basic sequence: (1) Precise monitoring of the initial calorimeter temperature drift with the resistance thermometer, (2) accurate measurement of the energy input for a predetermined time interval, and (3) again monitoring the calorimeter temperature in the final drift period until reaching quasi-adiabatic conditions.

Upon completion of the initial series of measurements (77 K to room temperature), the sample was again cooled to 77 K. The pressure on the nitrogen in the lower reservoir was then reduced gradually to solidify the liquid nitrogen at 63 K. By increasing the pumping rate on the solid nitrogen, the temperature of the lower reservoir was reduced to about 46 K. Heat capacity measurements were then made in the range 48 to 80 K. After completion of this series, the nitrogen in the lower reservoir was allowed to warm enough to melt at 63 K and then forced out by pressurizing with helium gas. The lower reservoir was filled with liquid helium via a vacuum-jacketed transfer tube. The calorimeter and adiabatic shield were positioned to contact the helium reservoir and cooled to 4.2 K in about 2.5 hours.

The sample of $CuO \cdot CuSO_4$ was then lowered into the measuring position, and the control shields were trimmed to achieve adiabatic conditions. Heat capacity measurements were taken up to about 16 K using the germanium thermometer. This series of runs was continued above 16 K with the platinum thermometer to approximately 48 K. The calorimeter was again cooled to the vicinity of 17 K, and another series of closer spaced measurements was made covering the range of anomalous Cp values.

The low-temperature experimental data of copper oxysulfate are listed in table 1, and shown graphically in figure 3. Heat capacity values are expressed in terms of the defined thermochemical calorie, 1 calorie = 4.1840 joules. These experimental molal heat capacities (Cex) were calculated using the equation

$$Cex = \frac{1}{m} \frac{i \int Edt}{4.184\ (\Delta T)} - Ce \pm k, \qquad (1)$$

where i = average heater current, amp;

m = moles sample,

$\int Edt$ = heater voltage-time integral for the heating period, volt-sec,

ΔT = corrected temperature rise,

Ce = Cp of empty calorimeter,

and k = collective term consisting of various corrections such as curvature, helium, and sample impurities.

Curvature corrections (16) were calculated from relationship

$$C - Cm = \frac{-(\Delta T)^2}{24} \frac{d^2C}{dT^2}, \qquad (2)$$

where C is the actual heat capacity in the measured interval and Cm is the mean heat capacity that is equal to the first term of the Cex equation. The second derivative of C, $\frac{d^2C}{dT^2}$, is assumed to be approximately equal to $\frac{d^2Cm}{dT^2}$.

The helium gas correction was 0.00047 cal/K, and was independent of sample temperature.

TABLE 1. - Experimental low-temperature heat capacities of $CuO \cdot CuS_2$ (s)

T, K	Cp, cal/deg-mole	T, K	Cp, cal/deg-mole
5.78	0.228	43.46	6.572
6.26	.258	47.40	7.375
7.03	.311	51.41	8.155
7.97	.389	53.50	8.554
9.00	.468	57.52	9.346
10.09	.591	62.18	10.268
11.16	.730	64.95	10.789
12.25	.908	68.56	11.450
12.48	.953	71.96	11.947
13.69	1.205	80.94	13.463
14.82	1.513	85.94	14.284
15.91	1.872	88.95	14.701
16.95	2.309	95.30	15.523
17.96	2.864	103.64	16.567
19.10	3.747	113.07	17.736
		123.23	18.941
17.42	2.552	133.76	20.133
18.28	3.080	144.78	21.309
18.67	3.331	155.98	22.441
19.10	3.726	164.70	23.298
19.56	4.272	174.20	24.180
19.97	4.703	185.37	25.191
20.07	3.971	197.09	26.246
20.51	3.330	208.55	27.189
21.28	1,705	220.17	28.161
22.26	2.390	231.90	28.993
20.27	3,675	243.68	29.849
		249.18	30.256
20.70	3.084	258.53	30.913
23.20	2.506	268.04	31.523
26.17	2.964	277.82	32.182
29.27	3.552	287.50	32.721
32.56	4.240	297.07	33.392
35.88	4.964	306.55	33.980
39.51	5.737		

Experimental data were smoothed using a digital computer and a curve fitting program developed by Justice (7). This program uses a least-squares procedure to approximate a data fit with orthogonal polynomic functions which results in equations of the general form:

$$Cp = A + BT + CT^2 + DT^3 + \ldots$$

The low-temperature Cp data were best fitted by dividing the temperature range 0 to 300 K into several segments. An overlap of about 10 K was used in joining the segments.

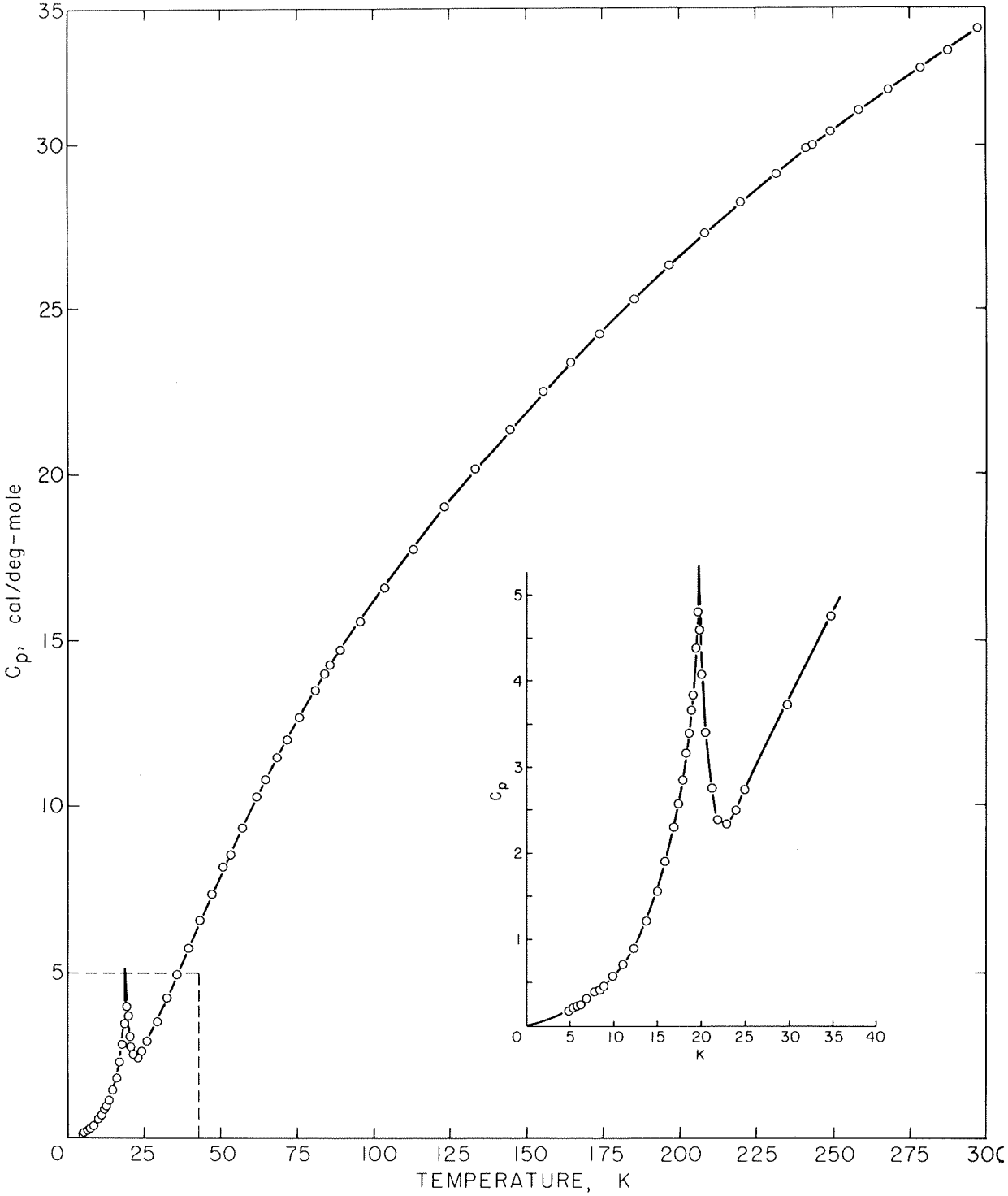

FIGURE 3. - Low-temperature heat capacity, $CuO \cdot CuSO_4$(s).

Table 2 lists the smoothed heat capacity data as well as the derived values of absolute entropy, the Gibbs free energy function, and the enthalpy referenced to 0 K. The entropy and enthalpy functions were computer-evaluated by numeric integration of the appropriate analytic functions derived from the curve-fitting routine. The entropy and enthalpy at 5 K were calculated by graphical extrapolation of a Cp/T versus T^2 plot to 0 K. The orthogonal fitting procedure was not suited for approximating the Cp curve in the transition zone. This portion of the data, 15 to 25 K, was graphically smoothed, and the corresponding entropy and enthalpy increments were calculated by Simpson's rule

TABLE 2. - Low-temperature thermodynamic properties of $CuO\text{-}CuSO_4$ (s)[1]

T, K	Cal/deg mole			$H^\circ - H_O^\circ$, cal/mole
	Cp°	S°	$-(G^\circ/H_O^\circ)/T$	
5	(0.19)	(0.13)	(0.052)	(0.39)
10	.58	.36	.143	2.17
15	1.56	.75	.274	7.14
20	4.60	1.52	.476	20.88
25	2.73	2.12	.757	34.08
30	3.73	2.70	1.03	50.20
35	4.76	3.35	1.31	71.41
40	5.81	4.06	1.61	97.85
45	6.86	4.80	1.92	129.54
50	7.89	5.58	2.25	166.43
60	9.86	7.19	2.94	255.28
70	11.66	8.85	3.66	363.01
80	13.30	10.52	4.42	487.98
90	14.79	12.17	5.19	628.58
100	16.15	13.81	5.98	783.37
110	17.40	15.40	6.75	951.19
120	18.58	16.97	7.54	1,131.2
130	19.70	18.50	8.33	1,322.6
140	20.78	20.00	9.11	1,525.1
150	21.83	21.47	9.88	1,738.2
160	22.83	22.91	10.65	1,961.5
170	23.80	24.32	11.41	2,194.7
180	24.73	25.71	12.71	2,437.4
190	25.63	27.06	12.92	2,689.2
200	26.48	28.41	13.66	2,949.8
210	27.31	29.72	14.39	3,218.8
220	28.11	31.01	15.12	3,495.9
230	28.88	32.27	15.83	3,780.9
240	29.62	33.52	16.55	4,073.4
250	30.33	34.74	17.25	4,373.2
260	31.01	35.95	17.95	4,679.9
270	31.65	37.12	18.64	4,993.3
280	32.28	38.29	19.32	5,312.9
290	32.92	39.43	19.99	5,638.9
298.15	33.45	40.36	20.53	5,909.4
300	33.57	40.56	20.66	5,971.4

[1]Values in parentheses are extrapolations.

The average deviation of the computer fit from the experimental data was ±0.01 Cp unit between 5 and 15 K, and ±0.03 Cp unit between 25 and 300 K. The maximum probable error in the Cp measurements was estimated to be approximately twice the average deviations in their respective ranges. A National Bureau of Standards standard Al_2O_3 sample was measured in the temperature range 50 to 300 K to check the relative accuracy of the low-temperature calorimeter. The measured heat capacities agreed within a 0.1-percent uncertainty range with those published by Furukawa (4) of the National Bureau of Standards.

ENTHALPY OF FORMATION

The formation energy of copper oxysulfate from its elements was obtained by solution calorimetry. The necessary sequence of reactions is outlined in table 3. Experimental apparatus and techniques involved are discussed elsewhere (10, 14).

TABLE 3. - Calorimetric reaction scheme for $CuO \cdot CuSO_4$ (s)

	Reaction	$\Delta H_{298.15}$, kcal	Uncertainty, ± kcal
(1)	$8H_2O(1) = 8H_2O(sol)$.....	-0.61	0.001
(2)	$CuO \cdot CuSO_4$ (s) + $4H^+$ (sol) = $2Cu^{++}$ (sol) + H_2SO_4 (sol) + H_2O(sol).....	-21.82	.02
(3)	$H_2SO_4 \cdot 7.0H_2O(1) = H_2SO_4 \cdot 7.0H_2O(sol)$.....	-.79	.02
(4)	$2CuO(s) + 4H^+(sol) = 2Cu^{++}(sol) + 2H_2O(sol)$...	-25.16	.06
(5)	$2CuO(s) + H_2SO_4 \cdot 7.0H_2O(1) = CuO\ CuSO_4$ (s) + $8H_2O(1)$..... $\Delta H_5 = -\Delta H_1 - \Delta H_2 + \Delta H_3 + \Delta H_4$	-3.52	.07
(6)	$2Cu(s) + O_2(g) = 2CuO(s)$.....	-74.40	.300
(7)	$H_2(g) + 2O_2(g) + S(rh) + 7H_2O(1) = H_2SO_4 \cdot 7.0H_2O(1)$.....	-209.46	.100
(8)	$H_2(g) + 1/2\ O_2(g) = H_2O\ (1)$.....	-68.32	.010
(9)	$2Cu(s) + S(rh) + 5/2\ O_2(g) = CuO \cdot CuSO_4$ (s).... $\Delta H_9 = \Delta H_5 + \Delta H_6 + \Delta H_7 - \Delta H_8$	-219.1	.3

Approximately 20 millimole samples of copper oxysulfate were dissolved in a "basic" quantity of 2,133.4 g of 4.36-molal HCl. The composition of this solvent corresponds to $HCl \cdot 12.731\ H_2O$. The reaction scheme required the experimental evaluation of the heats of solution of H_2O, $CuO \cdot CuSO_4$, $H_2SO_4 \cdot 7.0H_2O$ (7.93 m H_2SO_4), and CuO. Six solution determinations were made with each of these substances. The corresponding heats of reaction and assigned uncertainty are listed for these compounds in the first four

equations in table 3. Reaction 5 is the composite value of the preceding reactions and has a net heat value of -3.52±0.07 kcal.

Enthalpies for reactions 6, 7, and 8 were obtained from values selected by King, Mah, and Pankratz (8) for CuO and data compiled by Wagman (15) for H_2O and aqueous H_2SO_4. The uncertainties assigned equations 7 and 8 were estimated. The standard enthalpy formation of copper oxysulfate expressed by reaction 9 results in a value of -219.1±0.3 kcal/mole at 298 K.

DISCUSSION

The adiabatic calorimeter described in this investigation has wide-range applicability for accurate evaluation of absolute entropies. The theoretical basis for the validity of the calorimetric method was first postulated by Nernst in 1906. After considerable experimental confirmation, his statements and later works of Planck were refined into a basic concept now referred to as the Third Law of Thermodynamics (9). While there are notable exceptions, for example H_2O, most pure crystalline substances conform to third-law behavior; that is, their entropy approximates zero as the absolute temperature approaches zero. In addition to evaluating entropies, the adiabatic calorimeter has excellent capability for delineating energy effects accompanying many types of transitions, particularly when the rate of change is relatively slow.

In the present work the standard entropy at 298.15 K, $S°_{298.15}$ of copper oxysulfate was derived from heat capacity data measured in the temperature range 6 to 307 K using the relationship

$$S°_{298.15} = \int_{5}^{298.15} C_p d\ln T + 0.13. \qquad (3)$$

The 0.13 entropy unit is the extrapolated portion of entropy extending from 0 to 5 K. The lambda-type thermal anomaly observed in its heat capacity at 19.95 K probably results from an antiferromagnetic transition. The pretransition zone begins between 10 to 15 K and merges again with the "normal" Cp curve between 25 and 30 K. By comparison, Stout (13) observed a thermal anomaly in anhydrous cupric sulfate occurring at 34.8 with a pretransition zone appearing about 20 K.

The lattice entropy was estimated at 25 K and compared to the measured value. The difference was 0.56 cal/deg mole, which is considerably less than the $\Delta S°$ value predicted by a magnetic contribution of R$\ln$2.

The formation data of copper oxysulfate over an extended range of temperature are summarized in table 4. The standard entropy of formation $\Delta S°$ at 298 K was calculated using an entropy for Cu(s) from King, Mah, and Pancratz (8); S(r) and O_2(g) values were taken from JANAF (2). Combining the enthalpy of formation, -219.1±0.3 kcal/mole, the corresponding Gibbs energy of formation ($\Delta S°$) was calculated as -187.61 kcal/g-mole. The formation data above 298 K came from enthalpy data reported by Ferrante (4) based on high-temperature drop-calorimeter measurements. The standard formation data for

$CuO \cdot CuSO_4$ can be combined with other literature data to provide enthalpies and Gibbs energies for several reactions of metallurgical interest by which the oxysulfate can be formed. These are given in table 5. The Gibbs energy values for the reactions

$$2CuO + SO_3 = CuO \cdot CuSO_4$$

and

$$2CuSO_4 = CuO\ CuSO_4 + SO_3$$

are in excellent agreement with the recent equilibrium pressure measurements of Ingraham (5).

TABLE 4. - Thermodynamic properties of $CuO \cdot CuSO_4$ (s) to 1,200 K

[Formation: $2Cu(s) + 5/2O_2(g) + S(s,l) = CuO \cdot CuSO_4(s)$]

T, K	Cal/deg mole			Kcal/mole			Log Kf
	Cp°	S°	$-(G^\circ - H^\circ_{298})/T$	$H^\circ - H^\circ_{298}$	ΔHf°	ΔGf°	
0	0	0	∞	-5.91	-216.4	-216.4	∞
100	16.15	13.81	65.11	-5.13	-217.8	-208.1	454.80
200	26.48	28.41	43.21	-2.96	-218.8	-197.9	216.26
298.15	33.45	40.36	40.36	0	-219.1	-187.6	137.51
300	33.57	40.57	40.37	.06	-219.1	-187.4	136.52
350	36.01	45.93	40.79	1.80	-219.1	-182.1	113.71
[1]368.54	36.81	47.81	41.08	2.48	-219.1	-180.2	106.86
368.54	36.81	47.81	41.08	2.48	-219.2	-180.2	106.86
[2]388.36	37.63	49.76	41.47	3.22	-219.2	-178.1	100.23
388.36	37.63	49.76	41.47	3.22	-219.6	-178.1	100.23
400	38.09	50.88	41.73	3.66	-219.6	-176.8	96.60
450	39.87	55.47	43.00	5.61	-219.6	-171.5	83.29
500	41.38	59.75	44.47	7.64	-219.6	-166.1	72.60
550	42.64	63.75	46.04	9.74	-219.5	-160.8	63.90
600	43.70	67.51	47.68	11.90	-219.3	-155.5	56.64
650	44.59	71.05	49.34	14.11	-219.1	-150.2	50.50
700	45.33	74.38	51.01	16.36	-218.9	-144.9	45.24
[3]717.8	45.57	75.52	51.60	17.17	-218.8	-143.0	43.54
800	46.54	80.51	54.32	20.95	-	-	-
900	47.59	86.06	57.55	25.66	-	-	-
1,000	48.74	91.13	60.66	30.47	-	-	-
1,100	50.28	95.84	63.64	35.42	-	-	-
1,200	52.46	100.30	66.51	40.55	-	-	-

[1]Rhombic-monoclinic transition point of sulfur.
[2]Melting point of sulfur.
[3]Boiling point of sulfur.

TABLE 5. - Formation reactions of $CuO \cdot CuSO_4$ (s)

T, K	Kcal/mole		Log K	T, K	Kcal/mole		Log K
	ΔH°	ΔG°			ΔH°	ΔG°	
$CuO(s) + CuSO_4(s) = CuO \cdot CuSO_4(s)$							
298.15	1.80	0.61	-0.447	700	1.51	-0.87	0.272
300	1.80	.60	-.437	800	1.37	-1.20	.328
400	1.74	.21	-.115	900	1.20	-1.52	.369
500	1.63	-.17	.074	1,000	1.01	-1.81	.396
600	1.60	-.53	.193	1,100	.82	-2.08	.413
$2CuO(s) + SO_3(g) = CuO\ CuSO_4(s)$							
298.15	-50.12	-37.79	27.701	800	-48.75	-17.65	4.822
300	-50.12	-37.71	27.472	900	-48.38	-13.78	3.346
400	-49.97	-33.60	18.358	1,000	-47.96	-9.96	2.177
500	-49.73	-29.53	12.908	1,100	-47.96	-6.18	1.228
600	-49.43	-25.52	9.296	1,200	-46.86	-2.46	.448
700	-49.10	-21.56	6.731				

REFERENCES

1. Comite International des Poids et Mesures (The International Committee on Weights and Measures). The International Practical Temperature Scale of 1968. Metrologia, v. 5, No. 2, 1969, pp. 35-44.

2. Dow Chemical Co., Thermal Research Laboratory. JANAF Thermochemical Tables, Second Edition. N.S.R.D.S., NBS 37, SN03030872, U.S. Government Printing Office, Washington, D.C., 1971, 1141 pp.

3. Ferrante, M. J. Enthalpies and Entropies Above 298.15° K for Copper Sulfate and Copper Oxysulfate. BuMines RI 7600, 1972, 8 pp.

4. Furukawa, G.T., T. B. Doughlas, R. E. McCoskey, and D. C. Ginnings. Thermal Properties of Aluminum Oxide From 0 to 1,200 K. J. Res., NBS, v. 57, No. 2, 1956, pp. 67-82.

5. Ingraham, T. R. Thermodynamics of the Thermal Decomposition of Cupric Sulfate and Cupric Oxysulfate. Trans. AIME, v. 233, No. 2, 1965, pp. 359-363.

6. International Union of Pure and Applied Chemistry, Division of Inorganic Chemistry, Commission on Atomic Weights. Atomic Weights of the Elements (1969). Pure and Appl. Chem., v. 21, 1970, pp. 97-108.

7. Justice, B. H. Thermal Data Fitting With Orthogonal Functions and Combined Table Generation. The FITAB Program. Univ. Mich., Ann Arbor, Mich., COO-1149-143, 1969, 49 pp.

8. King, E. G., A. D. Mah, and L. B. Pankratz. Thermodynamic Properties of Copper and Its Inorganic Compounds. INCRA Monograph II, 1973, 257 pp.

9. Lewis, G. N., and M. Randall. Thermodynamics and the Free Energy of Chemical Substances. McGraw-Hill Book Co., Inc., New York, 1923, 653 pp.

10. Mrazek, R. V., D. W. Richardson, H. O. Poppleton, and F. E. Block. Determination of the Heat of Formation of Vanadium Trichloride. BuMines RI 7096, 1968, 15 pp.

11. Riddle, J. L., G. T. Furukawa, and H. H. Plumb. Platinum Resistance Thermometry. NBS Monograph 126, April 1973, 129 pp.

12. Sparks, L. L., R. L. Powell, and W. J. Hall. Preference Tables for Low-Temperature Thermocouples. NBS Monograph 124, June 1972, 61 pp.

13. Stout, J. W. Thermal Anomaly in Anhydrous Copper Sulfate. J. Chem. Phys., v. 9, No. 3, 1941, p. 285.

14. Stuve, J. M., L. B. Pankratz, and D. W. Richardson. Thermodynamic Properties of $(Na_2O)_4$ Fe_2O_3, 6° to 1,200° K. BuMines RI 7535, 1971, 12 pp.

15. Wagman, D. D., W. H. Evans, V. B. Parker, I. Halow, S. M. Bailey, and R. H. Schumm. Selected Values of Chemical Thermodynamic Properties. NBS Tech. Note 270-3, January 1968, 263 pp.

16. Westrum, E. F., Jr., G. T. Furukawa, and J. P. McCullough. Adiabatic Low-Temperature Calorimetry. Ch. 5 in Experimental Thermodynamics, v. 1, Calorimetry of Non-Reacting Systems, ed. by J. P. McCullough and D. C. Scott. Butterworths, London, 1968, pp. 133-214.

☆ U.S. GOVERNMENT PRINTING OFFICE: 1975-603-752/27 INT.-BU.OF MINES,PGH.,PA. 20269